Catalysis Today 423 (2023) 114297

Contents lists available at ScienceDirect

Catalysis Today

journal homepage: www.elsevier.com/locate/cattod

Understanding the formation of higher alcohols in the liquid-phase ethanol condensation over copper-loaded hydrotalcite-derived mixed oxides

Laura Faba [a], Jennifer Cueto [b], Ma Ángeles Portillo [c], Ángel L. Villanueva-Perales [c], Fernando Vidal-Barrero [c], Salvador Ordóñez [a,*]

[a] Catalysis, Reactors and Control Research Group (CRC), Dept. of Chemical and Environmental Engineering, University of Oviedo, 33006 Oviedo, Spain
[b] IMDEA Energy Inst, Thermochem Proc Unit, Avda Ramón de la Sagra 3, Móstoles, Madrid 28935, Spain
[c] Departamento de Ingeniería Química y Ambiental, Universidad de Sevilla, Camino de los Descubrimientos, s/n., Sevilla 41092, Spain

ARTICLE INFO

Keywords:
Guerbet reaction
1-Octanol
2-Ethyl-1-hexanol
Schultz-Flory distribution
Alcohol coupling
Step growth

ABSTRACT

The production of higher alcohols ($C_{\geq 4}$) via ethanol liquid-phase condensation over different Cu-based catalysts is studied in this work. Experimental results demonstrate that dehydrogenation steps are more relevant than hydrogenation steps, according to the lack of improvement in activity when a bimetallic (Pd-Cu) catalyst. Thus, the sequential hydrogenation via Meerwein-Ponndorf-Verley (MPV) and surface-mediated H-transfer is identified as active enough to obtain the desired alcohols. The best results were obtained with a 20 % Cu/MgAl catalyst, showing more than 10 % of ethanol conversion (free solvent conditions) and 60 % selectivity to higher alcohols (16 % to C6 and C8 ones). Experiments with different feed compositions, including C4 alcohols and acetaldehyde, and a comprehensive analysis of all the results in terms of a mechanistic oligomerization model, demonstrate that the C-C coupling follows a step-growth model where the condensation between monomers coexists with the one involving oligomers.

1. Introduction

Alcohols with four to eight carbons (generally known as higher alcohols) have a relevant industrial value as solvents, chemical intermediates, and fuel oxygenate additives [1–3]. Nowadays, they are commercially produced from olefins in a multistep process of oxo-hydrocarbonylation, and subsequent hydrogenation and separation steps, using petroleum feedstock as the raw material [4]. This production route and, subsequently, the market of these alcohols, has an inherent dependency on oil prices and a very high carbon footprint. The development of alternative and sustainable routes, not involving fossil resources, is nowadays of key interest.

Ethanol is one of the most evident platform molecules for these purposes, taking advantage of the well-established industrial production processes and the expected decrease in the light fuel demand, which guarantees its availability and suggests the development of alternative technologies to upgrade this chemical [5–8].

In this context, the condensation of renewable CO_2-neutral ethanol to obtain higher alcohols could be an interesting alternative. Different groups have studied this reaction, known as the Guerbet condensation [9], without reaching a full agreement about the reaction mechanism, and mainly focused on 1-butanol synthesis. Thus, some authors propose the direct condensation of two alcohols [10], whereas other researchers defend the route via the dimerization of alcohol with its aldehyde [11] or the condensation of alcohol with its enol [12]. However, the most accepted pathway is known as the "indirect" mechanism, a three-step route involving the coexistence of dehydrogenations, condensations, and, finally, reductions to obtain the higher alcohols [13–15]. This complexity requires the development of multifunctional catalysts, combining basic or acidic properties (to promote condensation) with hydrogenation/dehydrogenation active phases (usually, metal sites). There is a general agreement about ethanol dehydrogenation (acetaldehyde production) as the rate-limiting step of the process, highlighting the role of acidic sites [16–18]. When using basic-acidic catalysts (such as oxides [11,19], hydrotalcite-derived oxides [15,20,21], and hydroxyapatites [22,23]), the alcohols production in absence of any noble metal follows a sequential route involving the Meerwein-Ponndorf-Verley (MPV) mechanism (C═O bonds hydrogenation) and the surface-mediated H-transfer (C═C bonds hydrogenation) [24]. However, the reaction rates of these hydrogenations are

* Corresponding author.
E-mail address: sordonez@uniovi.es (S. Ordóñez).

https://doi.org/10.1016/j.cattod.2023.114297
Received 1 March 2023; Received in revised form 6 July 2023; Accepted 17 July 2023
Available online 19 July 2023

significantly lower than the metal-promoted hydrogenations [25,26], and these acidic sites also promote undesired etherification and esterification reactions, with the subsequent reduction in selectivity [15]. Thus, a balance trade-off between the catalytic properties is needed, with most of the studies considering reaction in gas phase (>300ºC) to reach the required activity and focused on the 1-butanol production [13, 27].

In the last years, the interest has been extended to secondary coupling reactions to produce $C_{\geq 6}$ alcohols. As in the case of those studies focused on 1-butanol, the production of $C_{\geq 6}$ alcohols is mainly studied in the gas phase [24,28–30]. However, it is expected that working in the condensed phase, at high pressure and close to the ethanol critical point, the product distribution control increases, being easier to identify the predominant reaction mechanism and, subsequently, the catalytic properties required to enhance the selectivity to the target alcohols. This approach, however, has been scarcely studied [14,31–33]. The sustainability of some of these studies is questionable since pressures up to 176 bar and temperatures of 250–300ºC are proposed [33], or the reaction is performed using toluene as solvent [32].

In our case, we propose a free-solvent reaction (pure ethanol) and a more moderate pressure (30 bar of N_2). After a complete catalytic screening presented in our previous study [31], Cu/MgAl is identified as the most promising material to produce $C_{\geq 6}$ alcohols (6.8 % of ethanol conversion after 8 h at 230ºC, 50 % selectivity to alcohols with >18 % of C6s and C8s). The promising results obtained with this metal, leads us to consider testing larger Cu loading on the mixed oxides. Despite the relevant conclusions about the reaction mechanism extracted, conversions and selectivities obtained are far to be competitive in comparison to other studies in the gas phase.

This work optimizes this approach to maximize ethanol conversion and alcohol productivity, and looks for a further understanding of the reaction, mainly looking at the formation of heavier alcohols ($\geq C_6$). Increasing the metal and catalytic loading, working with bimetallic materials and mechanical mixtures of different catalysts, co-feeding different intermediates, and considering the influence of a reducing atmosphere are evaluated as possible reaction improvements. A deep analysis of the experimental data demonstrates that the reaction network of all condensation pathways, independently of the catalyst used, matches the predictions of a step-growth polymerization model. These polymerization models have been recently applied to the study of gas-phase condensation reactions, as poly(oxomethylene)-dimethylether [34], as well as to ethanol Guerbet reactions [24,29]. However, this work is the first that, to the best of our knowledge, applied this procedure to liquid phase reactions.

2. Material and methods

2.1. Catalysts preparation

The MgAl support (MgAl = 2/1) was prepared in the lab by the co-precipitation in a 0.1 M of an aqueous solution of Na_2CO_3 of two 1 M solutions of $Mg(NO_3)_2{\cdot}6\ H_2O$ and $Al(NO_3)_2{\cdot}9\ H_2O$ salts added in a 2/1 molar ratio (both salts supplied by Sigma Aldrich, >98 wt %). The crystallization occurs at 85ºC under 300 rpm of stirring. The mixture was aged for 24 h, filtered, centrifuged, and washed several times to remove the remaining sodium cations. The solid obtained was dried overnight and sieved (50–80 μm). The hydrotalcite obtained was then calcined in air flow (100 mL·min^{-1}) with a temperature slope of 5ºC·min^{-1}, holding the final temperature (700ºC) for 5 h.

Bifunctional catalysts were prepared using copper nitrate as the metal precursor, using a solution with the corresponding amount of salt to guarantee the target concentration of the metal, 1 or 20 wt %, in the final material. The volume used, according to the dry impregnation method used, corresponded to the pore volume of the support, ensuring total impregnation and good dispersion. In the case of the bimetallic catalyst, a second impregnation step was performed, using the same method to introduce a 1 wt % Pd nitrate solution on the 20 % Cu/MgAl surface. The impregnated materials were dried and calcined at the same conditions as the support, and reduced in an H_2 flow of 20 mL·min^{-1} at 450ºC (temperature slope of 5ºC·min^{-1}), holding this temperature for 3 h. Impregnation procedures for incorporating Cu ions were selected, instead of adding the metal during the coprecipitation steps, in order to keep unchanged, as far as possible, the acid and basic sites distributions of the parent MgAl oxides.

2.2. Catalysts characterization

The catalytic morphology was analyzed by N_2 physisorption (Micromeritics ASAP 2020), applying the BET and BJH methods to calculate the surface area and the pore volume, respectively. The metal loading was determined by Inductively Coupled Plasma Mass Spectrometer (ICP-MS) using an HP7900. The metal dispersion and average particle size of 20 % Cu catalyst were defined by X-ray diffraction (PANalytical X'Pert Pro), working with the Cu-Kα line (0.154 nm) in the range 2θ= 10–120ºC and applying the Scherrer equation to the metal most intense peak obtained in the diffractograms. In the case of 1 % Cu-catalyst, the dispersion was obtained by TEM using a MET JEOL 1011 apparatus, and the software Confocal ImageJ for calculating the histograms and average particle size distribution.

The acidity and basicity were determined by a programmed temperature desorption (TPD) analysis carried out in a Micromeritics AutoChem II 2920. After a cleaning step with He, the surface was saturated by flowing 20 mL·min^{-1} of 2.5 % NH_3/He or 99.5 % of CO_2, to measure the acidity and basicity, respectively. The desorption of these probe molecules was monitored (Pfeiffer Vacuum-300 mass spectrometer) from room temperature to 950ºC, with a slope of 5ºC·min^{-1}.

2.3. Ethanol condensation

The ethanol liquid phase condensation was carried out in a 0.5 L autoclave reactor (Autoclave Engineers EZE Seal) using 200 mL of ethanol (VWR, 100 %) and 0.5 or1 g of catalyst (depending on the experiment). The air was purged with N_2 and the temperature was increased up to 230ºC after pressuring with 30 bar of N_2 (inert conditions) or 25 bar of N_2 and 5 bar of H_2 (reductive conditions) reaching final pressures at the operation temperature of about 80 bar. The reaction was performed under a fast stirring (1000 rpm), to avoid the presence of external mass transfer limitations.

The evolution of the compounds involved was analyzed by GC-FID (Shimadzu GC-2010) using a 30 m long CP-SIL 8 CB capillary column and commercial samples for the identification of the main compounds involved. When needed, the identification of the peaks was assisted by a GC-MS (Shimadzu GC/MS QP 2010 Plus Instrument) with the same column and analytical program. All the data shown correspond to the average value of three analyses, obtaining a standard deviation lower than 5 % in all the cases. These data were analyzed according to the parameters defined in Eqs. 1–3, where "n_i" corresponds to the number of carbons in each compound, and "$C_{i,t}$" is the molar concentration of this compound at the time analyzed:

$$Selectivity: \varphi(\%) = \frac{n_i \cdot C_{i,t}}{2 \cdot \left([EtOH]_0 - [EtOH]_t\right)} \cdot 100 \quad (1)$$

$$Conversion: x \quad (\%) = \frac{[EtOH]_0 - [EtOH]_t}{[EtOH]_0} \cdot 100 \quad (2)$$

$$Carbon \quad Balance: CB = \frac{\sum n_i \cdot C_{i,t}}{2 \cdot [EtOH]_0} \quad (3)$$

To qualitatively check the formation of gaseous by-products, gas samples were periodically taken using sampling bags. GC-MS analyses of these samples show that ethylene is the only permanent gas formed during the reaction.

3. Results and discussion

3.1. Catalyst screening

The first set of liquid-phase (ethanol without any additional solvent) experiments were performed with the two Cu-modified catalysts used in this work (1 % Cu/MgAl and 20 % Cu/MgAl, with two different catalytic loadings, 2.5 and 5 g/L), being the results obtained after 8 h reaction time summarized in Fig. 1. The activity of the parent MgAl oxide has been deeply analyzed in our previous work [31], and also depicted in this figure for comparison purposes. The positive role of Cu is observed, both in terms of conversion and alcohol selectivity.

When introducing 1 % of Cu, the conversion is more than five times higher than in absence of this metal. One of the most relevant effects of this rise in conversion is the higher acetaldehyde selectivity (from 2.5 % to 18.8 %). This increase could be anticipated considering the well-known dehydrogenation activity of Cu [29]. These Cu nanoparticles enable an increase in the concentration of surface H and allow the transport of such species across the catalyst surface. The H-transfer capability increases the rate of deprotonation of the β-C of ethanol, obtaining the acetaldehyde. In the same way, the higher selectivity to butanal (the main component of the C4 aldehydes fraction) obtained with 1 %Cu/MgAl (2.9 %, almost 10 times higher than with the parent MgAl) could be explained by the combination of the H removal in deprotonation of the β-C of butanol and the hydrogenation of the β-C of crotonaldehyde. The complete distribution of all the products detected is included in the Supplementary Information (Table S1).

Although the highest selectivity to alcohols is obtained with MgAl (79.1 %), the presence of Cu leads to a clear increase in the carbon length of these target compounds, reaching 10.5 % of C6 alcohols (less than 1 % obtained with MgAl). The low metal loading hardly affects the basic/acidic properties of the parent material, see Table 1 (all the results summarized in Table 1 are detailed in the Supplementary Information, Fig. S1-S4), and the total selectivity for C6 compounds are quite similar in both cases (11.3 % with MgAl, 12.7 % with 1 % Cu/MgAl, in selectivity terms).

The high discrepancy in the alcohols/aldehydes ratio is explained by the increase in the hydrogenation rate due to the H_2 produced by the H removal promoted by the copper nanoparticles.

Cu addition also has negative consequences, since this metal also catalyzes lateral reactions of decarbonylation and esterification, obtaining undesired products, both in the liquid and the gas phase, compounds that account for 18 % of the total selectivity (in carbon basis). The main reaction products obtained from non-condensation reactions are ethyl acetate, butyl acetate, and diethoxyethane. The first two compounds are formed by dehydrogenative coupling reactions, catalyzed by transition metals as Cu [35,36]. In good agreement with this fact, both the selectivity to these undesired liquid by-products, and the relative weight of the esters in this mix, increases with Cu loadings.

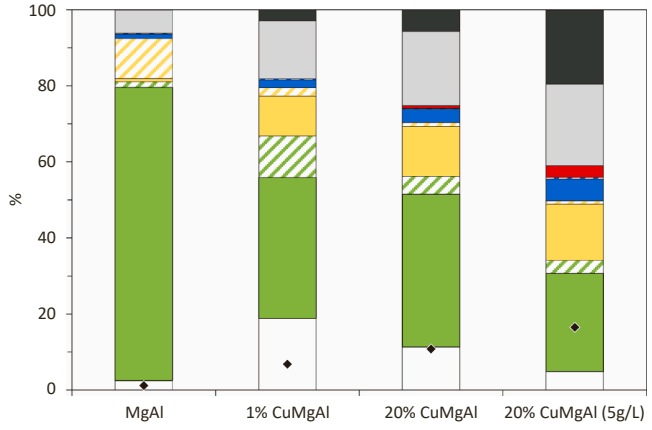

Fig. 1. Ethanol conversion and selectivity to products after 8 h of ethanol self-condensation at 230ºC, and 2.5 g/L of catalyst loading (unless otherwise stated). Data correspond to ethanol conversion (◆); and selectivity to: acetaldehyde (white); butanol (green); C4 aldehydes (green stripes); C6 alcohols (yellow); C6 aldehydes (yellow stripes); C8 alcohols (blue); C10 alcohols (red); undesired liquid compounds (grey); gas products (black).

Table 1
Surface and physicochemical properties of the different metal modified Mg/Al (2/1) catalysts. Results corresponding to N_2 physisorption, NH_3 and CO_2-TPD, ICP, TEM, and XRD.

	MgAl	1 % Cu/MgAl	20 % Cu/MgAl	1 %Pd20 %Cu/MgAl
S_{BET} ($m^2 \cdot g^{-1}$)	179	173	58	56
v_p ($cm^3 \cdot g^{-1}$)	0.62	0.45	0.26	0.23
Total acidity (μmol·g^{-1})	**1857**	**1491**	**765**	**695**
Weak (<250ºC)	726	436	230	166
Medium	959	606	410	437
Strong (>500ºC)	172	449	125	92
Total basicity (μmol·g^{-1})	**716**	**598**	**513**	**495**
Weak (<250ºC)	185	324	130	139
Medium	441	210	270	233
Strong (>500ºC)	90	65	113	123
Metal loading (wt%)	–	0.96	19.7	0.98 (Pd) 19.7 (Cu)
Metal dispersion (%)	–	24.2	4.5	4.5
Metal crystallite size (nm)	–	5.2*	23.4**	25 (Cu)***

*Measured by TEM
** Measured by XRD
*** Cu crystallite size measured by XRD. The Pd signal could not be distinguished with clarity enough to evaluate it.

In global terms, the catalyst 1 % Cu/MgAl demonstrates a higher activity for ethanol condensation, reaching 0.24 mol/L of total higher alcohols, a value significantly higher than the 0.14 mol/L obtained with the parent MgAl.

Based on these preliminary analyses, and considering the acetaldehyde production is a determinant step in the reaction pathway, the possibility of increasing the metal loading was evaluated, testing the activity of 20 % Cu/MgAl. An unexpectedly low increase in conversion is observed, from 6.8 % to 10.8 %, but the distribution of the products indicates a positive effect on the production of higher alcohols. Thus, the selectivity to this family of compounds reaches a value of 61 % (relative increment of 23 % for the value obtained with 1 % Cu/MgAl), obtaining increases in all the fractions: from 37 % to 41 %, and from 10 % to 13 %, for C_4 and C_6 alcohols, respectively. A significant amount of C8 and C10 alcohols are also detected, with a global selectivity of 4.3 %. As in the previous case, a relevant role of Cu nanoparticles enhancing undesired reactions is observed, with almost 20 % of esters and acetals, with a proportional increase in gaseous and liquid components. In global terms, this catalyst allows producing 0.45 mol/L of higher alcohols, almost two times the value obtained with the low Cu loading catalyst, suggesting a higher activity of the 20 % Cu material (increase in productivity higher than the increase in conversion).

The slight increase in conversion could be explained based on the chemical properties of this material (Table 1). The presence of metal nanoparticles blocks part of the acidic and basic sites of the support, this effect being significantly more evident in the case of 20 % Cu/MgAl, mainly in terms of acidity. This result suggests a preferential deposition of the metal on the acidic sites of the MgAl during the synthesis. According to the most accepted mechanism, the condensation is catalyzed by Brønsted basic sites [37], but the role of acidity is very relevant to stabilize the acetaldehyde and the resulting condensed intermediate, a stabilization that requires the dehydration of this compound (acidic mechanism).

Considering this, a particular experiment using twice catalytic

loading (from 2.5 to 5 g/L) was performed, the most relevant results being shown in Fig. 1. A significant increase in ethanol conversion is observed (from 10.8 % to 16.5 %) as well as changes in the distribution of the products. The mixture is enriched in higher alcohols (24 % of C6, C8, and C10s), a value that represents a relative increase of 36.2 % concerning the total selectivity obtained when using the low catalytic loading. In addition, the butanol selectivity significantly decreases, from 40.2 % to 25.8 %, because of the prevalence of lateral reactions that compete with the main condensation route. In fact, more than 40 % of undesired gaseous and liquid compounds are obtained. With this global situation, using a double amount of catalyst only represents an increment of 25 % on the total amount of alcohols obtained, this approach being discarded for future studies.

Alternatively, the option to evaluate a bimetallic catalyst was considered, choosing the 20 %Cu/MgAl to disperse a nominal amount of 1 % of Pd. This second metal is introduced considering its high hydrogenation activity [38], to maximize the hydrogenation of aldehydes to target alcohols. This catalyst was tested at two different reaction conditions: in inert atmosphere and in reducing one (5 bar of H_2), the main results are plotted in Fig. 2.

The use of the bimetallic catalyst does not change the ethanol conversion, reaching final values after 8 h of 9.6 %, and 10.2 %, in inert and reducing atmospheres, respectively. These values differ by less than 6 % the value obtained with 20 %Cu/MgAl (10.8 %) being justified by the similar concentration of basic/acid pairs of both materials (see Table 1) and the negligible role of hydrogen-promoting condensations. The expected improvement in the distribution of the products is not obtained. In inert atmospheres, the distribution by families according to the carbon number is very similar (10.8 % of C2, 36.4 % of C4, 13.4 % of C6, 5.1 % of C8, and 2.7 % of $C_{>8}$, see Table S1 for the complete distribution), highlighting the decrease in the C4 fraction in favor of a higher selectivity to undetected gaseous compounds obtained by decarbonylation (15.7 %). In the case of C4 compounds, the alcohols/aldehydes ratio significantly decreases, from 8.6 to 3.8. This result suggests two possible situations: low activity of Pd nanoparticles in inert atmosphere because of the low hydrogen concentration available, or a preferential deposition of Pd nanoparticles on the Cu surface, decreasing the Cu dehydrogenation activity and, subsequently, the available H_2.

A tighter control on the reaction selectivity is reached when working in a reducing atmosphere, with an absence of undesired gases produced by decarbonylation. The same total selectivity of target alcohols as when using 20 %Cu/MgAl is obtained, 57.7 %, but is enriched in the heaviest fractions (2.5 % of C10, 6 % of C8, and 15.3 % of C6 alcohols). In global terms, the improvements obtained are not relevant enough to justify the use of palladium and reducing conditions (with the subsequent increase in operating costs).

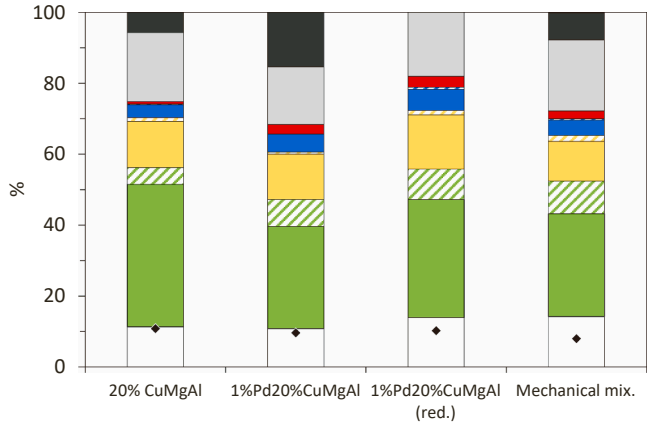

Fig. 2. Ethanol conversion and selectivity to products after 8 h of ethanol self-condensation at 230ºC using different catalyst and catalytic configurations. Data correspond to ethanol conversion (◆); and selectivity to: acetaldehyde (white); butanol (green); C4 aldehydes (green stripes); C6 alcohols (yellow); C6 aldehydes (yellow stripes); C8 alcohols (blue); C10 alcohols (red); undesired liquid compounds (grey); gas products (black).

In conclusion, the 20 % Cu/MgAl is considered as the optimum catalyst. However, experimental results suggest that the improvement in activity because of the dehydrogenation capacity of Cu nanoparticles is partially shielded by the decrease in the concentration of basic/acidic active pairs concerning the support. This fact explains the increase in the acetaldehyde selectivity observed when using Cu materials, suggesting that, under these conditions, condensation could be the rate-limiting step. Based on this assumption, a mechanical mixture of MgAl and Cu/MgAl was considered. A similar total amount of solid catalyst as in previous experiments (0.5 g) was used, combining 0.25 g of each material. The main results are analyzed in Fig. 2, with the complete distribution of all the products detected being included in Table S1.

The conversion obtained (8 %) is slightly higher than the theoretical conversion that could be anticipated with both contributions, suggesting a synergetic effect. This result would indicate that Cu does not need to be atomically close to acid-base sites, the acetaldehyde produced on the Cu surface being capable to migrate to a basic/acidic pair to continue reacting. This behavior has been previously suggested by Cuello-Penaloza et al. [29] when considering the ethanol condensation in the gas phase using low-Cu loading catalysts. However, the distribution of the products obtained in this case demonstrates that most of this ethanol converted is transformed into undesired liquids and gaseous products. The decarbonylation and esterification that produce these products are catalyzed by Cu nanoparticles [29], which suggests a low migration capacity of this acetaldehyde. This result is congruent with the high metal loading and the lower mobility expected when working in the condensed phase.

As to the products of the main pathway, the mechanical mixture does not result in a significant improvement, except for the slight increase observed for the heaviest alcohols, with 2.2 % of $C_{>8}$. This fraction was not detected with MgAl and only appears as traces with 20 %Cu/MgAl. In global terms, the mechanical mixture produces a total alcohols selectivity of 46.7 % with a selectivity to aldehydes (25.5 %) similar to the one obtained with the bimetallic catalyst. These results discard the use of a mechanical mixture as a good approach to enhance alcohols production, reinforcing the identification of 20 %Cu/MgAl as the best catalyst.

To ensure that deactivation does not affect the kinetic studies performed in the subsequent Section, a catalyst reusability test has been performed for the 20 % Cu/MgAl catalyst. After a reaction test performed at the abovementioned conditions (5 g/L of catalyst, 230ºC, 200 mL of ethanol, 8 h reaction time), the content of the reactor was filtered to recover the catalyst. The catalyst was washed with acetone and dried overnight at 110ºC, repeating the reaction cycle with this recovered catalyst. The same procedure was repeated for four cycles. The conversions were very similar in the four cases ($16^{+}/_{-}2$ %, without systematic trends), whereas the selectivity pattern was the same that the observed in the Fig. 1 for the 20 % Cu/MgAl.

This fact is a good agreement with the characterization results obtained for the MgAl oxides and 1 % Cu/MgAl, used for this reaction [31]. Characterization of the used catalysts showed that morphology (BET analysis) and crystallinity of the catalysts (XRD) remains unchanged during the reaction, the presence of metal leaching is discarded, and the variations observed in the acid and basic distribution (lower concentration, shift the weaker strengths) seemed to be or related to the initial surface reconstruction of the catalyst surface with the ethanol, rather than to any deactivation effect [31].

3.2. *Reaction pathway and kinetic modelling*

Fig. 3 shows the temporal evolution of the ethanol conversion and the total concentration of higher alcohols (C4-C12) obtained with all the catalysts and configurations analyzed in this work. As suggested by these

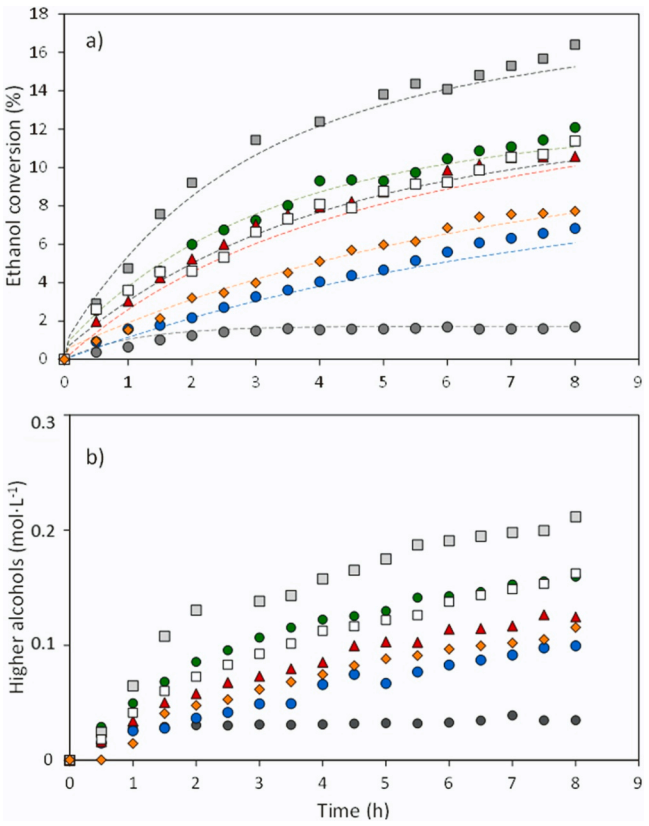

Fig. 3. : Temporal evolution of ethanol self-condensation at 230ºC analysed in terms of (a) ethanol conversion, and (b) higher alcohols concentration (C4-C12). Data correspond to: (●) MgAl, (●) 1 % Cu/MgAl; (●) 20 % Cu/MgAl; (●) 20 % Cu/MgAl (5 g/L); (▲) 1 %Pd20 %Cu/MgAl; (□) 1 %Pd20 %Cu/MgAl (reducing atmosphere); and (◆) mechanical mixture of MgAl and 20 % Cu/MgAl.

temporal profiles, except when using MgAl, longer reaction times would produce better results, both in terms of conversion and alcohols yields. Reactions were performed for a constant reaction time of 8 h because results at this time are relevant enough to highlight the differences between the studied catalytic systems and to establish the main conclusions about the reaction mechanism and kinetic.

The ethanol consumption has been fit to a first-order kinetic model considering two parallel reactions, the main route of ethanol decomposition by dehydrogenation and subsequent reactions (k_1) and the undesired acid-catalyzed dehydration reactions yielding ethylene (k_2). Diethyl ether, the other dehydration product that could be obtained from ethanol is not detected in any experiment. Seeing the complexity of the reaction (more than twelve compounds identified), this simplified kinetic fit was performed on a carbon basis, considering all the compounds derived from acetaldehyde together. Broken lines observed in Fig. 3 correspond to this fit, whereas the kinetic rate constants and the coefficients of determination of the regressions are presented in Table 2.

Table 2
Kinetic rate constants of ethanol consumption reactions and coefficients of determination of the regressions.

Catalyst	k_1 (h^{-1})	k_2 (h^{-1})	r^2
MgAl	0.011	0.005	0.9998
1 % Cu/MgAl	0.012	0.001	0.9997
20 % Cu/MgAl	0.037	0.002	0.9997
20 % Cu/MgAl (5 g/L)	0.052	0.004	0.9994
1 %Pd20 %Cu/MgAl	0.026	0.004	0.996
1 %Pd20 %Cu/MgAl (red.)	0.028	0.005	0.997
MgAl + 20 %Cu/MgAl	0.015	0.001	0.9999

The kinetic rate constant of the undesired reactions directly involving the ethanol molecule (k_2), is largely lower for the considered catalysts. According to this, the role of the catalyst is mainly focused on promoting the main pathway. In good agreement with the previous analysis, the highest kinetic rate constant was obtained with 20 % Cu/MgAl, whereas a low improvement is observed when comparing the bimetallic catalyst in an inert or reducing atmosphere. Although a perfect correlation is not obtained, the k_1 values decrease with the acidity of these materials (Fig. S5). These results demonstrate that the activity of the Cu nanoparticles prevails over the surface properties of the support.

The temporal distribution of all the compounds follows the same trend, independently of the catalyst used. For example, Fig. 4 shows the evolutions obtained with 20 % Cu/MgAl (the others being included in the supplementary information, Fig. S6 and S7). According to the indirect mechanism, the fast increase of acetaldehyde could be anticipated since ethanol dehydration is the first step required. This result, as well as the flat profile observed after 2 h (production and consumption are in balance), suggests that this compound is the intermediate involved in the condensation, discarding a relevant role of the ethanol's direct self-condensation. The same behavior that the acetaldehyde is observed with the rest of the aldehydes (butanal, crotonaldehyde, hexanal), in all the cases with the maximum reached at longer times and with lower concentrations. On the contrary, all alcohols follow an increasing trend, the typical behavior of final products.

These results suggest that the subsequent condensation steps directly occur from the corresponding aldehydes, with a negligible role of alcohols direct condensation or butanol dehydrogenation. Based on these conclusions, the ethanol condensation follows the general mechanism proposed in Scheme 1. This mechanism is in good agreement with the previous literature [30,31].

As previously mentioned, the acetaldehyde plays a key role in the ethanol condensation with MgAl-derived catalysts, in good agreement with the most accepted mechanism in which the C-C coupling requires a multistep process, involving ethanol dehydrogenation, aldol condensation, and sequential MPV and surface-mediated hydrogenation steps to obtain the 1-butanol [16]. The same sequence of steps could be applied to the following condensations, reaching C6 and C8 alcohols. However, this chain-growth mechanism can be categorized as either monomer-oligomer coupling (if it implies always adding an acetaldehyde unit to a previous monomer or oligomer), oligomer-oligomer coupling (if the initial dehydrogenation could affect directly to 1-butanol units), or a mixture of both options. The results obtained using ethanol as a reactant do not allow distinguishing between these pathways.

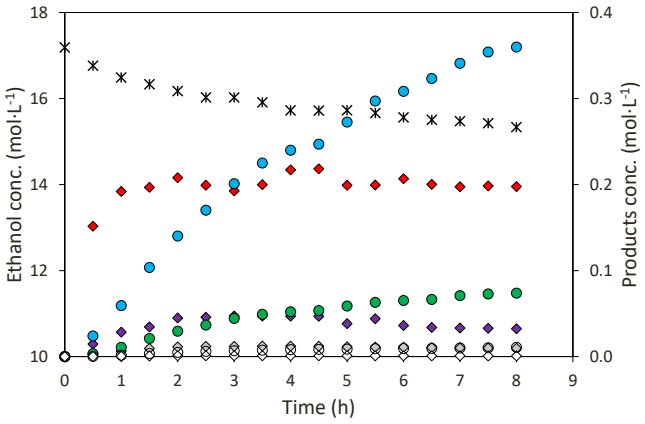

Fig. 4. : Temporal evolution of different compounds involved in the liquid-phase ethanol (*) condensation at 230ºC using 20 % Cu/MgAl (2.5 g/L) as the catalyst. Symbols: (◆) acetaldehyde; (●) butanol; (◆) butanal; (●) crotonaldehyde *(overlapped by the C6-aldehydes)*; (●) C6-alcohols; (◆) C6-aldehydes; (○) C8-alcohols; (◇) C8-aldehydes.

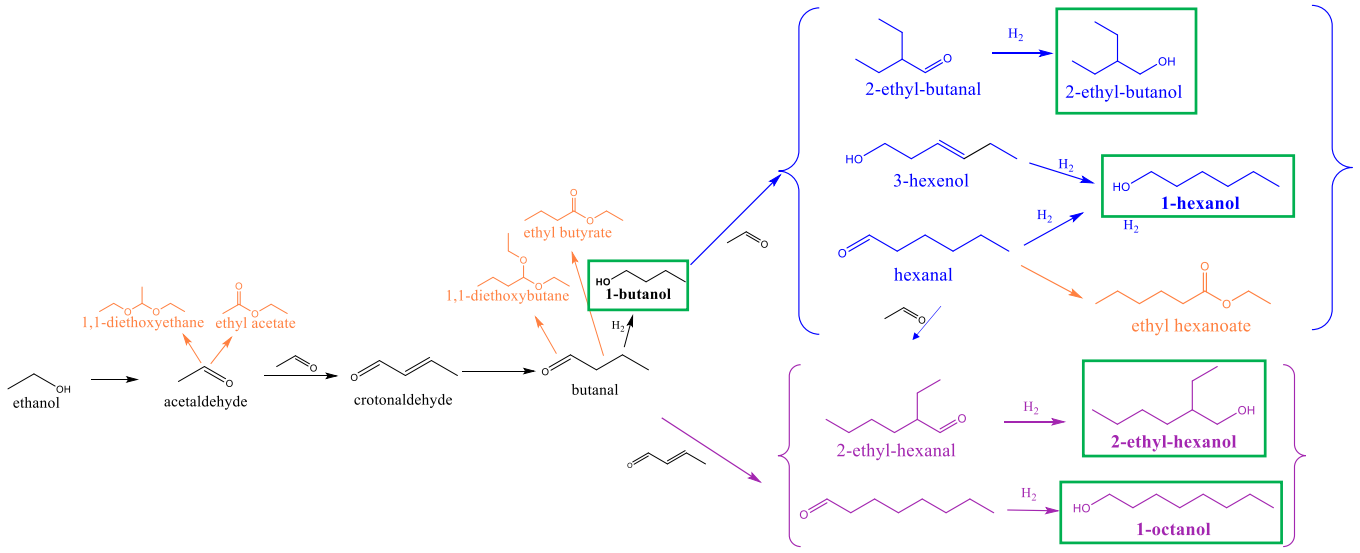

Scheme 1. : Proposed scheme for the ethanol liquid-phase condensation. Green squares correspond to condensation alcohols; blue and purple letters to condensation aldehydes and orange compounds to the "undesired liquid products" lump in the discussions.

To evaluate the relative weight of each mechanism in this reaction, experiments co-feeding ethanol and acetaldehyde or 1-butanol (90 % of ethanol, 10 % of acetaldehyde or butanol, both on a volume basis) as the reactants were performed. The main results obtained after 8 h are shown in Fig. 5. The conversion can be only analysed for ethanol since both acetaldehyde and 1-butanol act as reactants and products.

The ethanol conversion increases when co-feeding acetaldehyde (from 10.8 % to 13.7 %). Despite the difficulty to define the conversion of acetaldehyde, final samples indicate a net decrease of 84 %, which indicates a fast consumption of this compound. The high availability of this aldehyde and the enrichment in heavier fractions (more than 11 % of C8 alcohols) suggests the prevalence of a monomer-oligomer coupling mechanism, where acetaldehyde plays a key role. This hypothesis agrees with the results obtained with the mixture of ethanol and butanol. In this case, the absence of acetaldehyde justifies the lack of improvement in terms of conversion (10.5 %). This result also indicates that there is competitive adsorption of butanol, ethanol, and acetaldehyde on the same types of active sites, with butanol more weakly adsorbed than ethanol and acetaldehyde, in such a way that the butanol that oligomerizes is mainly the one in-situ produced, its condensation taking place before its desorption to the liquid phase.

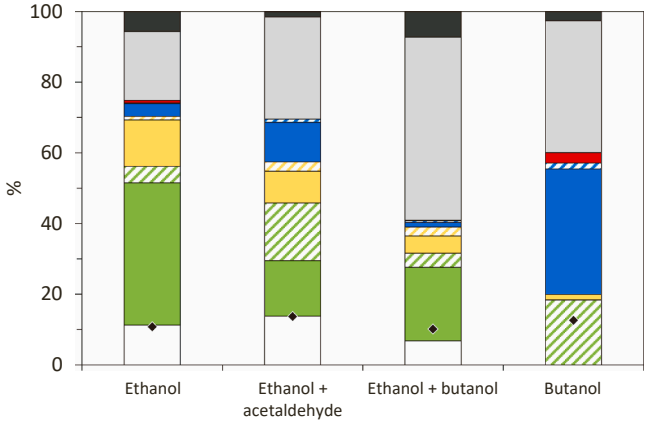

Fig. 5. Summary of main results obtained after 8 h of reaction at 230ºC using 20 %Cu/MgAl as a function of the reactant mixture used. Data correspond to ethanol conversion (◆); and selectivity to: acetaldehyde (white); butanol (green); C4 aldehydes (green stripes); C6 alcohols (yellow); C6 aldehydes (yellow stripes); C8 alcohols (blue); C10 alcohols (red); undesired liquid compounds (grey); gas products (black).

The situation is significantly different when this competition disappears because there is not any ethanol or acetaldehyde in the medium. When feeding butanol (last column of Fig. 5), 12.6 % of conversion is obtained, with a very relevant selectivity to C_8 alcohols (35.5 %), an almost total absence of C6 alcohols (1.5 %), and a relevant amount of butanal (18.4 %). In addition, the $C_{>8}$ fraction of alcohols is due to C_{12} compounds (2-butyl-1-octanol and 2-ethyl-1-decanol), being in all the cases multiple of four carbons. These results suggest that, in absence of ethanol, the butanol is adsorbed on the active sites, its dehydrogenation being possible and the condensation produced mainly by the interaction of two butanal molecules or the corresponding oligomer with another butanal unit. Concerning to the undesired liquid reaction products, the pattern observed when feeding the ethanol-containing mixtures is very similar to the one obtained with pure ethanol (being ethyl acetate the main compound of this family). In the presence of acetaldehyde, the butyl acetate selectivity is almost twice, which correlates with the larger concentration of C4 aldehydes. Butyl butyrate is the main non desired compound, followed by other esters (hexanoates, octanoates) when using butanol as feed.

As indicated before, this behaviour is only observed in absence of C_2 compounds whereas the carbon-chain growth in presence of ethanol preferentially follows a monomer-oligomer mechanism, where the acetaldehyde is the monomeric unit, at least for low ethanol conversions. To corroborate this hypothesis, the experimental results were analysed considering polymerization models [39]. Thus, the progress of the different reactions (α) was described by the fractional consumption of the initial number of reactive groups (-C═O) according to Eq. 4, where $N_0$is the number of ethanol molecules and N_{2i} is the number of reactive groups remaining among all the molecules with a carbon number of C_{i2} after a given extension of the reaction:

$$\alpha = \frac{(N_0 - \sum N_{2i})}{N_0} \quad (4)$$

Fig. 6 shows the strong and well-defined dependence of α on the ethanol conversion, being possible to evaluate the data as a function of the two limiting cases; (1) fast monomer self- and cross-coupling (i.e., all the condensations being marked by the addition of an acetaldehyde molecule); and (2) fast oligomer self-coupling (all the C8 alcohols being produced by the condensation of two crotonaldehyde units).

Experimental values are far from this second option, discarding this

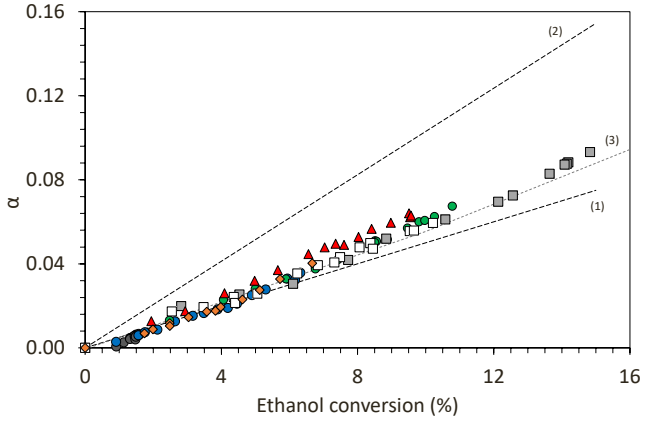

Fig. 6. : Experimental values of the fractional consumption of the initial number of reactive groups (α) as a function of the ethanol conversion obtained at 230ºC with: (●) MgAl, (●) 1 % Cu/MgAl; (●) 20 % Cu/MgAl; (●) 20 % Cu/MgAl (5 g/L); (▲) 1 %Pd20 %Cu/MgAl; (□) 1 %Pd20 %Cu/MgAl (reducing atmosphere); and (◆) mechanical mixture of MgAl and 20 % Cu/MgAl. The broken lines represent the three theoretical models: (1) condensation governed by monomer coupling (k_{m-m}, $k_{m-o} >> k_{o-o}$), (2) reactions between oligomers ($k_{o-o} >> k_{m-m}$, k_{m-o}); and (3) all condensation steps have similar rate constants ($k_{m-m} = k_{o-o} = k_{m-o}$).

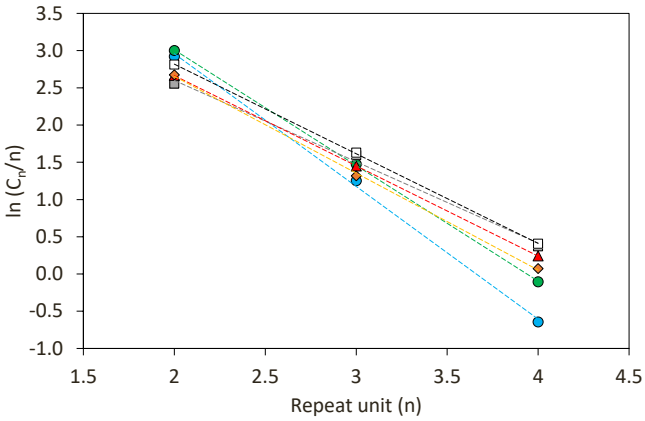

Fig. 7. Shultz-Flory distribution plots for alcohols. Data correspond to: (●) 1 % Cu/MgAl; (●) 20 % Cu/MgAl; (●) 20 % Cu/MgAl (5 g/L); (▲) 1 %Pd20 %Cu/MgAl; (□) 1 %Pd20 %Cu/MgAl (reducing atmosphere); and (◆) mechanical mixture of MgAl and 20 % Cu/MgAl.

possibility as the chain-growth mechanism. Values at conversions lower than 8 % match with the first model, suggesting that the oligomerization via acetaldehyde addition is the only route. These results correspond to values obtained with MgAl, 1 %Cu/MgAl, and the rest of the catalysts tested at initial times. However, for those catalysts with higher Cu loading (higher dehydrogenation capacity) and, mainly, for ethanol conversions higher than 8 %, the trend outlined by the experimental values diverges from this limiting model, being closer to an intermediate situation where all condensation steps have similar rate constants. This behaviour has been previously observed by Flaherty and co-workers, in this case studying the ethanol gas-phase condensation using hydroxyapatite-based catalysts [24]. The theoretical line that defines this third situation (3) overlaps line (1) for low conversions with a polynomic evolution and, subsequently, an increasing deviation for this line as the conversion increases.

The behaviour defined by line (3) is commonly identified as step-growth polymerization [39], and it is based on the Flory statement known as The Equal Reactivity Principle: "the intrinsic reactivity of all functional groups is constant, independent of the molecular size" [39]. To corroborate if this Principle is applicable in this case, the equation of the Schultz-Flory model is considered for the last points, where the selectivity distributions are quite stable (t = 6–8 h). This model is defined by Eq. 5, where "n" is the repeat unit defined as ethanol, "C_n" is the carbon selectivity of the alcohols with n-repeat units, "α" is the chain-growth probability (the probability of an adsorbed C_n alcohol chain to grow to C_{n+1}), and (1- α) is the desorption probability, i.e., the probability of obtaining a C_n alcohol product [40]. The results are plotted in Fig. 7.

$$\ln\left(\frac{C_n}{n}\right) = (n-1)\cdot\ln(\alpha) + 2\cdot\ln(1-\alpha) \quad (5)$$

As observed in Fig. 7, the alcohol selectivities fit the Schultz-Flory model despite the catalyst used (r^2 = 0.995–1). Data corresponding to MgAl were not included since, the lack of any dehydrogenation active phase in this material minimizes the concentration of higher alcohols, maximizing the possible errors in a logarithmic distribution. In good agreement, this material has the lowest α value (α = 0.07), suggesting that almost the total amount of butanol obtained is desorbed. The highest growth probability is obtained with 20 %Cu/MgAl with double catalytic loading of 5 g/L (α = 0.34). This coefficient decreases to 0.21 when using this catalyst in a concentration of 2.5 g/L, this value being slightly lower than those reached with the bimetallic catalyst (α = 0.30, despite the inert or reducing atmosphere), or when using the mechanical mixture (α = 0.27). These results demonstrate the prevalence of basic-acidic pair activity over the hydrogenation one (Pd). In the cases of 1 % Cu/MgAl and the mechanical mixture (MgAl + 20 %Cu/MgAl), intermediate α values were obtained (0.17 and 0.27, respectively).

4. Conclusions

20 % Cu/MgAl is demonstrated to be a promising catalyst to obtain higher alcohols by liquid-phase ethanol condensation. With this material, more than 56 % of higher alcohols were obtained after 8 h, with 11 % of ethanol conversion (solvent-free configuration). No relevant improvements are observed when introducing a bimetallic catalyst, concluding that Cu is active enough to promote the hydrogenation of the condensed products by the MPV and surface-mediated H-transfer mechanisms.

Competitive adsorption of ethanol, butanol and acetaldehyde on the active sites explains the key role of acetaldehyde in the final distribution of products. Thus, the condensation of butanol units is mainly possible for the butanol in situ produced, suffering dehydrogenation before its release.

A deep mechanistic analysis of experimental data demonstrates that all the results, independently of the catalyst or catalytic system used, match the predictions of a step-growth polymerization model where the condensation between monomers coexists with the one involving oligomers.

CRediT authorship contribution statement

Laura Faba: methodology, supervision, data curation, writing-original draft, **Jennifer Cueto:** Investigation, **M. Angeles Portillo:** review, **Angel Luis Villanueva Perales:** review, **Fernando Vidal Barrero:** formal analysis, funding, **Salvador Ordóñez:** Conceptualization, supervision, formal analysis, writing-review.

Declaration of Competing Interest

The authors declare that they have no known competing financial interests or personal relationships that could have appeared to influence the work reported in this paper.

Data Availability

Data will be made available on request.

Acknowledgments

This work has been carried out in the framework of the Project BIOC4+(PY18-RE-0040) funded by Junta de Andalucía and European Union (ERDF funds). Authors would like to acknowledge the technical support provided by Servicios Científico-Técnicos de la Universidad de Oviedo.

Appendix A. Supporting information

Supplementary data associated with this article can be found in the online version at doi:10.1016/j.cattod.2023.114297.

References

[1] B. Rajesh Kumar, S. Saravanan, Use of higher alcohol biofuels in diesel engines: a review, Renew. Sustain. Energy Rev. 60 (2016) 84–115, https://doi.org/10.1016/j.rser.2016.01.085.
[2] T. Tsuchida, S. Sakuma, T. Takeguchi, W. Ueda, Direct synthesis of n-butanol from ethanol over nonstoichiometric hydroxyapatite, Ind. Eng. Chem. Res. 45 (2006) 8634–8642, https://doi.org/10.1021/ie0606082.
[3] S.C. Patankar, G.D. Yadav, Cascade engineered synthesis of 2-ethyl-1-hexanol from n-butanal and 2-methyl-1-pentanol from n-propanal using combustion synthesized Cu/Mg/Mal mixed metal oxide trifunctional catalyst, Catal. Today 291 (2017) 223–233, https://doi.org/10.1016/j.cattod.2017.01.008.
[4] E.S. Olson, R.K. Sharma, T.R. Aulich, Higher-alcohols biorefinery, Appl. Biochem. Biotechnol. 113 (2004) 913–932, https://doi.org/10.1385/abab:115:1-3:0913.
[5] N.M. Eagan, M.D. Kumbhalkar, J.S. Buchanan, J.A. Dumesic, G.W. Huber, Chemistries and processes for the conversion of ethanol into middle-distillate fuels, Nat. Rev. Chem. 3 (2019) 223–249, https://doi.org/10.1038/s41570-019-0084-4.
[6] J. Sun, Y. Wang, Recent advances in catalytic conversion of ethanol to chemicals, ACS Catal. 4 (2014) 1078–1090, https://doi.org/10.1021/cs4011343.
[7] P. Domenech, I. Pogrebnayakov, A.T. Nielsen, A. Riisager, Catalytic production of long-chain hydrocarbons suitable for jet-fuel use from fermentation-derived oxygenates, Green. Chem. 24 (2022) 3461–3474, https://doi.org/10.1039/d2gc00619g.
[8] C.E. Cabrera Camacho, A.L. Villanueva Perales, B. Alonso-Fariñas, F. Vidal-Barrero, P. Ollero, Assessing the economic and environmental sustainability of bio-olefins: the case of 1,3-butadiene production from bioethanol, J. Clean. Prod. 374 (2022), 133963, https://doi.org/10.1016/j.jclepro.2022.133963.
[9] P. Domenech, I. Pogrebnyakov, A.T. Nielsen, A. Riisager, Catalytic production of long-chain hydrocarbons suitable for jet-fuel use from fermentation-derived oxygenates, Green. Chem. 24 (2022) 3461–3474, https://doi.org/10.1039/d2gc00619g.
[10] D. Wang, Z. Liu, Q. Liu, Efficient conversion of ethanol to 1-butanol and C5-C9 alcohols over calcium carbide, RSC Adv. 9 (2019) 18941–18948, https://doi.org/10.1039/C9RA02568E.
[11] A.S. Ndou, N. Pint, N.J. Coville, Dimerisation of ethanol to butanol over solid-base catalysts, Appl. Catal. A 251 (2003) 337–345, https://doi.org/10.1016/S0926-860X(03)00363-6.
[12] J. Scalbert, F. Thibault-Starzyk, R. Jacquot, D. Morvan, F. Meunier, Ethanol condensation to butanol at high temperatures over a basic heterogeneous catalyst: how relevant is acetaldehyde self-aldolization, J. Catal. 311 (2014) 28–32, https://doi.org/10.1016/j.jcat.2013.11.004.
[13] X. Wu, G. Fang, Y. Tong, D. Jiang, Z. Liang, W. Leng, L. Liu, P. Tu, H. Wang, J. Ni, X. Li, Catalytic upgrading of ethanol to n-butanol: progress in catalyst development, ChemSusChem 11 (2018) 71–85, https://doi.org/10.1002/cssc.201701590.
[14] T.L. Jordison, C.T. Lira, D.J. Miller, Condensed-phase ethanol conversion to higher alcohols, Ind. Eng. Chem. Res. 54 (2015) 10991–11000, https://doi.org/10.1021/acs.iecr.5b02409.
[15] J. Quesada, L. Faba, E. Díaz, S. Ordóñez, Role of the Surface intermediates in the stability of basic mixed oxides as catalyst for ethanol condensation, Appl. Catal. A 542 (2017) 271–281, https://doi.org/10.1016.j.apcata.2017.06.001.
[16] J. Quesada, L. Faba, E. Díaz, S. Ordóñez, Tuning the selectivities of Mg-Al mixed oxides for ethanol upgrading reactions through the presence of transition metals, Appl. Catal. A 559 (2018) 167–174, https://doi.org/10.1016/j.apcata.2018.04.022.
[17] J. Pang, M. Zheng, L. He, L. Li, X. Pan, A. Wang, X. Wang, T. Zhang, Upgrading ethanol to n-butanol over highly dispersed ni_MgAlO catalysts, J. Catal. 344 (2016) 184–193, https://doi.org/10.1016/j.jcat.2016.08.024.
[18] F.C. Meunier, J. Scalbert, R. Thibault-Starzyk, Unraveling the mechanism of catalytic reactions through combined kinetic and thermodynamic analyses: application to the condensation of ethanol, 3445-350, Comptes Rendus. Chim. 18 (2015), https://doi.org/10.1016/j.crci.2014.07.002.
[19] A. Chieregato, J. Velasquez Ochoa, C. Bandinelli, G. Fornasari, On the chemistry of ethanol on basic oxides: revising mechanisms and intermediates in the Lebedev and Guerbet reactions, ChemSusChem 8 (2014) 377–388, https://doi.org/10.1002/cssc.201402632.
[20] K.V. Valihura, P.I. Kyriienko, A.K. Melnyk, O.V. Larina, S.O. Soloviev, Influence of acid-base properties of Mg-Al oxides systems on their catalytic characteristics in the process of gas-phase conversion of ethanol to 1-butanol, Theor. Exp. Chem. 57 (2021) 205–212, https://doi.org/10.1007/s11237-021-09689-z.
[21] M.A.P. Crespo, F. Vidal-Barrero, L. Azancot, T.R. Reina, M. Campoy, Insights on Guerbet reaction: production of biobutanol from bioethanol over a Mg-Al spinel catalyst, Front. Chem. 10 (2022), 945596, https://doi.org/10.3389/fchem.2022.945596.
[22] B.C. Zhou, W.C. Li, W.L. Lv, S.Y. Xiang, X.Q. Gao, A.H. Lu, Enhancing ethanol coupling to produce higher alcohols by tuning H-2 partial pressure over a copper-hydroxyapatite catalyst, ACS Catal. 12 (2022) 12045–12054, https://doi.org/10.1021/acscatal.2c03327.
[23] H. Brasil, A.F.B. Bittencourt, K.C.E.S. Yokoo, P.C.D. Mendes, L.G. Verga, K. F. Andriani, R. Landers, J.L.F. Da Silva, G.P. Valenca, Synthesis modification of hydroxyapatite surface for ethanol conversion: the role of the acidic/basic sites ratio, J. Catal. 404 (2021) 802–813, https://doi.org/10.1016/j.jcat.2021.08.050.
[24] T. Moteki, D.W. Flaherty, Mechanistic insight to C-C bond formation and predictive models for cascade reactions among alcohols on Ca- and Sr- hydroxyapatites, ACS Catal. 6 (2016) 4170–4183, https://doi.org/10.1021/acscatal.6b00556.
[25] X.X. Han, S.Q. Li, X.H. Zhu, H.L. An, X.Q. Zhao, Y.J. Wang, Influence of noble metals on the catalytic performance of Ni/TiO2 for ethanol Guerbet condensation, React. Kinet. Mech. Catal. 131 (2020) 919–933, https://doi.org/10.1007/s11144-020-01899-1.
[26] J. Quesada, L. Faba, E. Díaz, S. Ordóñez, Enhancement of the 1-butanol productivity in the ethanol condensation catalysed by noble metal nanoparticles supported on Mg-Al mixed oxide, Appl. Catal. A 563 (2018) 64–72, https://doi.org/10.1016/j.apcata.2018.06.037.
[27] A. Galadima, O. Muraza, Catalytic upgrading of bioethanol to fuel grade biobutanol: a review, Ind. Eng. Chem. Res. 54 (2015) 7181–7194, https://doi.org/10.1021/acs.iecr.5b01443.
[28] N.M. Eagan, M.P. Lanci, G.W. Huber, Kinetic modelling of alcohol oligomerization over calcium hydroxyapatite, Acs. Catal. 10 (2020) 2978–2989, https://doi.org/10.1021/acscatal.9b04734.
[29] P.A. Cuello-Penaloza, R.G. Dastidar, S.-C. Wang, Y. Du, M.P. Lanci, B. Wooler, C. E. Kliewer, I. Hermans, J.A. Dumesic, G.W. Huber, Ethanol to distillate-range molecules using Cu/MgxAlOy catalysts with low Cu loadings, Appl. Catal. B 304 (2022), 120984, https://doi.org/10.1016/j.apcatb.2021.120984.
[30] O.V. Larina, K.V. Valihura, P.I. Kyriienko, N.V. Vlasenko, D.Y. Balakin, I. Khalakhan, T. Cendak, S.O. Soloviev, S.M. Orlyk, Succesive vapour phase Guerbet condensation of ethanol and 1-butanol over Mg-Al oxide catalysts in a flow reactor, Appl. Catal. A 588 (2019), 117265, https://doi.org/10.1016/j.apcata.2019.117265.
[31] L. Faba, J. Cueto, M.A. Portillo, A.L. Villanueva Perales, S. Ordóñez, F. Vidal-Barrero, Effect of catalyst surface chemistry and metal promotion on the liquid-phase ethanol condensation to higher alcohols, Appl. Catal. A 643 (2022), 118783, https://doi.org/10.1016/j.apcata.2022.118783.
[32] M. Xue, B. Yang, C. Xia, G. Zhu, Upgrading ethanol to higher alcohols via biomass-derived Ni/bio-apatite, ACS Sust. Chem. Eng. 10 (2022) 3466–3476, https://doi.org/10.1021/acssuschemeng.1c07189.
[33] H.S. Ghaziaskar, C. Xu, One-step continuous process for the production of 1-butanol and 1-hexanol by catalytic conversion of bio-ethanol at its sub-/supercritical state, RSC Adv. 3 (2013) 4271–4280, https://doi.org/10.1039/c3ra00134b.
[34] R. Pelaez, P. Marín, S. Ordóñez, Synthesis of poly(oxymethylene) dimethyl ethers from methylal and trioxane over acidic ion exchange resins: a kinetic study, Chem. Eng. J. 396 (2020), 125305, https://doi.org/10.1016/j.cej.2020.125305.
[35] Z. Liu, J. Li, Y. Tan, L. Guo, Y. Ding, Copper supported on MgAlOx and ZnAlOx porous mixed-oxides for conversion of bioethanol via Guerbet coupling reaction, Catalysts 12 (2022) 1170, https://doi.org/10.3390/catal12101170.
[36] P. Benito, A. Vaccari, C. Antonetti, D. Licursi, N. Schiarioli, E. Rodriguez-Castellón, A.M.R. Galletti, Tunable copper-hydrotalcite derived mixed oxides for sustainable ethanol condensation to n-butanol in liquid phase, J. Clean. Product. 209 (2019) 1614–1623, https://doi.org/10.1016/j.jclepro.2018.11.150.
[37] Z. Wang, G. Lu, Y. Guo, Y. Guo, X.Q. Gong, Effect of one-pot rehydration process on surface basicity and catalytic activity of $Mg_yAl_{1-a}REE_aO_x$ catalyst for aldol condensation of citral and acetone, ACS Sus. Chem. Eng. 4 (2016) 1591–1601, https://doi.org/10.1021/acssuschemeng.5b01533.
[38] A. Molnar, A. Sarkany, M. Varga, Hydrogenation of carbon-carbon multiple bonds: chemo-, regio- and stereo-selectivity, J. Mol. Catal. A 173 (2001) 185–221, https://doi.org/10.1016/S1381-1169(01)00150-9.
[39] J.R. Fried. Polymer Science and Technology, 3rd ed..,, Prentice hall. Upper Saddle River,, NJ, 2014. ISBN: 0-8493-8939-9.
[40] C.T. Young, R. von Goetze, A.K. Tomov, F. Zaccaria, G.J.P. Britovsek, The mathematics of ethylene oligomerization and polymerization, Top. Catal. 63 (2020) 294–318, https://doi.org/10.1007/s11244-019-01210-0.